Magnetization density distribution in U_2Co_2Sn

1999 J. Phys.: Condens. Matter 11 2115

(http://iopscience.iop.org/0953-8984/11/9/008)

J. Phys.: Condens. Matter **11** (1999) 2115–2125. Printed in the UK PII: S0953-8984(99)97030-3

Magnetization density distribution in U_2Co_2Sn

J A Paixão†, L C J Pereira‡, P Estrela§, M Godinho§, M Almeida†, L Paolasini‖*, M Bonnet¶, J Rebizant+ and J C Spirlet+

† Departamento de Fisica, Facultade de Ciências e Tecnologia, Universidade de Coimbra, P-3000 Coimbra, Portugal

‡ Departamento de Quimica, Instituto Tecnológico e Nuclear, P-2686 Sacavém Codex, Portugal

§ Departamento de Fisica, Facultade de Ciências da Universidade de Lisboa, Campo Grande, Edificio C1, P-1700 Lisboa, Portugal

‖ Laboratoire Léon-Brillouin (CEA-CNRS), Centre d'Etudes Saclay, F-91191 Gif-sur-Yvette, France

¶ Departement de Recherche Fondamentale sur la Matière Condensée, SPSMS, F-38054 Grenoble Cédex 9, France

+ European Commission, Joint Research Centre, Institute for Transuranium Elements, Postfach 2340, D-76125 Karslruhe, Germany

Received 27 August 1998

Abstract. A magnetization density study by means of polarized-neutron scattering on the intermetallic compound U_2Co_2Sn is reported. U_2Co_2Sn belongs to the large An_2T_2X (An = U, Np, Pu, Am; T = transition metal; X = In, Sn) family of compounds crystallizing in an ordered variant of the tetragonal U_3Si_2 type of structure (space group $P4/mbm$). U_2Co_2Sn does not order magnetically but has a large magnetic susceptibility that qualifies it as an enhanced paramagnet or spin fluctuator. We report single-crystal magnetization measurements that show a significant magnetic anisotropy, with a c-axis susceptibility exceeding that measured on the basal plane by a factor of four. The magnetization density distribution in the unit cell was measured at 2 K by polarized-neutron scattering under a magnetic field of 5.5 T applied parallel to the c-axis. It was found that the major contribution to the magnetic susceptibility is located on the U atoms ($\mu_U = 118(3)\ m\mu_B$) but a small response from the Co atoms is also measured ($\mu_{Co} = 13(2)\ m\mu_B$).

1. Introduction

U_2Co_2Sn belongs to the isostructural family of An_2T_2X intermetallic compounds (An = U, Np, Pu, Am; T = transition metal; X = In, Sn) crystallizing in an ordered variant of the tetragonal U_3Si_2 structure (space group $P4/mbm$). Since its discovery (Péron *et al* 1993, Mirambet *et al* 1993), this family of compounds has attracted a great deal of interest. The electric and magnetic properties have been systematically studied, mainly for uranium polycrystalline samples. A broad range of magnetic behaviour is found, ranging from Pauli paramagnetism to antiferromagnetism with a sizable ordered f moment. Some of these compounds have heavy-fermion properties (Nakotte *et al* 1994, Havela *et al* 1995, Fukushima *et al* 1995) which partly explains the interest and justifies a thorough investigation of their physical properties.

These compounds have also been studied theoretically (Diviš *et al* 1994, 1995, 1997, Matar 1995). In most cases the magnetic ground-state properties (ordered as opposed to non-magnetic) are correctly predicted by band-structure calculations (Havela *et al* 1994). The

* Present address: European Synchrotron Radiation Facility, BP 220X, F-38043 Grenoble Cédex, France.

0953-8984/99/092115+11$19.50

calculations indicate that the hybridization of the f electrons with the d band of the ligands is responsible for the strong reduction of the 5f moment observed in some compounds, leading eventually to a paramagnetic or spin-fluctuation state. From these studies two basic findings have emerged:

(a) filling up the d band yields an increase of the degree of localization, i.e., a decrease of the f–d hybridization;
(b) the degree of localization increases with increasing U–X distance.

These trends in f–d hybridization are confirmed by experiment. For both systems (X = In, Sn) an increased tendency towards magnetic ordering is found upon filling the d band. U_2Co_2Sn is a spin-fluctuation system and lies on the border between paramagnetism (U_2Fe_2Sn) and ordered magnetism (U_2Ni_2Sn) and is thus a particularly interesting compound to investigate as regards the subject of f–d hybridization.

A controversial issue is the origin of the large magnetic anisotropy of these compounds. This anisotropy may originate from crystal-field effects but it may also be due partially to the energy involved in breaking an f–f or f–d bond, the so-called 'hybridization-induced' anisotropy. An interesting peculiarity of this family of compounds is that, depending on the T and X elements, the shortest inter-actinide distance can be found either along the *c*-axis or in the basal plane. For the closely related 1:1:1 UTX family of intermetallic compounds, it was found that the moment direction is always pointing perpendicular to the shortest U–U distance. Neutron diffraction studies have found evidence for a strong anisotropic f–d hybridization that might be responsible for the huge anisotropy energies (Paixão *et al* 1992, 1993). Exceptions to the shortest-f–f-distance rule have been found in the 2:2:1 family; U_2Rh_2Sn provides one of these exceptions. The shortest U–U distance (3.63 Å) in U_2Rh_2Sn is along the *c*-axis and yet magnetization and neutron diffraction measurements on a single crystal show that the moments align along $\boldsymbol{c}$ (Pereira *et al* 1996). Another exception is provided by the present compound, U_2Co_2Sn. The shortest U–U distance (3.512 Å) links two actinide atoms along $\boldsymbol{c}$ and the measurements reported below show that in this case also the easy-axis coincides with the unique tetragonal *c*-axis.

In the neutron diffraction study of the isostructural compound U_2Rh_2Sn (Pereira *et al* 1996) there was no evidence for an ordered moment associated with the Rh atoms, and a standard U^{3+} form factor could fit the data well. A much better sensitivity to any small moment transferred to the Rh site by hybridization between the f and d electrons could have been obtained using polarized neutrons. However, U_2Rh_2Sn orders antiferromagnetically with a wave-vector $\boldsymbol{\kappa} = (0, 0, 1/2)$ and a classical polarized-neutron diffraction experiment can only be performed in a $\kappa = 0$ magnetic structure. This is the case for ferromagnets and paramagnets, for which a strong enough magnetic field can induce a small magnetization parallel to the applied field. U_2Co_2Sn does not order magnetically, but has an enhanced magnetic susceptibility, as it is on the verge of magnetic ordering, and thus makes a good subject for such a precise polarized-neutron work.

2. Crystal growth and magnetization

The compound U_2Co_2Sn has been synthesized by arc melting under a purified argon atmosphere stoichiometric amounts of the metals with purities of at least 99.9% (U) and 99.999% (Co, Sn). A sample of ∼20 g of the molten alloy was encapsulated in a tungsten crucible and sealed by electron beam welding under vacuum (2×10^{-5} atm). Single crystals were grown using a technique known as *mineralization*. The tungsten crucible was held for a

week at a temperature slightly below the melting point (1140–1180 °C). The crystals used for the magnetization and neutron diffraction studies are from the same batch.

Magnetization measurements were performed on a small single crystal of ∼8 mg mass with approximate dimensions $2 \times 1 \times 1$ mm^3, using a Quantum Design SQUID magnetometer. The magnetization and susceptibility curves were measured along the main crystallographic *a*- and *c*-directions in the temperature range 2–200 K and in fields up to 5.5 T.

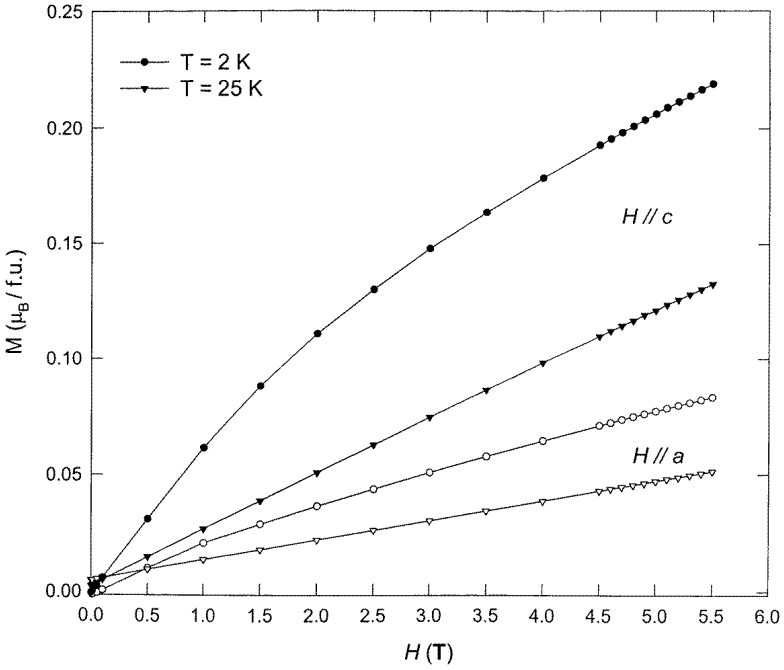

Figure 1. The field dependence of the magnetization density of a U_2Co_2Sn single crystal at 2, 5 and 25 K (open symbols: $\boldsymbol{H} \parallel \boldsymbol{a}$; solid symbols: $\boldsymbol{H} \parallel \boldsymbol{c}$).

The field dependence of the magnetization is shown in figure 1. In both directions, the $M(H)$ curves show the same approximately linear behaviour at temperatures above 25 K, typical of a paramagnetic state. At lower temperatures, the magnetization curves along $\boldsymbol{c}$ depart significantly from linear behaviour. At any temperature and for fields up to 5.5 T, the magnetization values along $\boldsymbol{c}$ are higher than those measured along $\boldsymbol{a}$, showing an important uniaxial magnetic anisotropy, which has been predicted by Nakotte *et al* (1994) from a comparison between free- and fixed-powder susceptibility measurements.

The susceptibility curves measured down to 2 K do not show any magnetic anomaly that could be associated with the onset of magnetic ordering (figure 2). Above 20 K the inverse susceptibility measured along the easy axis follows a Curie–Weiss law with $\Theta_p = -24.5$ K and an effective magnetic moment $\mu_{eff} = 1.65\,\mu_B$/U. Previously reported data for polycrystalline samples were fitted with a modified Curie–Weiss ($\chi = \chi_0 + C/(T + \Theta_p)$) law and the values $\Theta_p = -51$ K, $\mu_{eff} = 1.5\,\mu_B$/U and $\chi_0 = 2.3 \times 10^{-8}$ m^3 mol^{-1} were found. The larger value of μ_{eff} measured for a single crystal with the field applied along the easy axis compared to that obtained for polycrystalline samples is not unusual for systems with high magnetic anisotropy. For all directions, the low-temperature ($T < 20$ K) susceptibility values are higher than those given by the Curie–Weiss law extrapolated from the high-temperature range as shown in figure 2

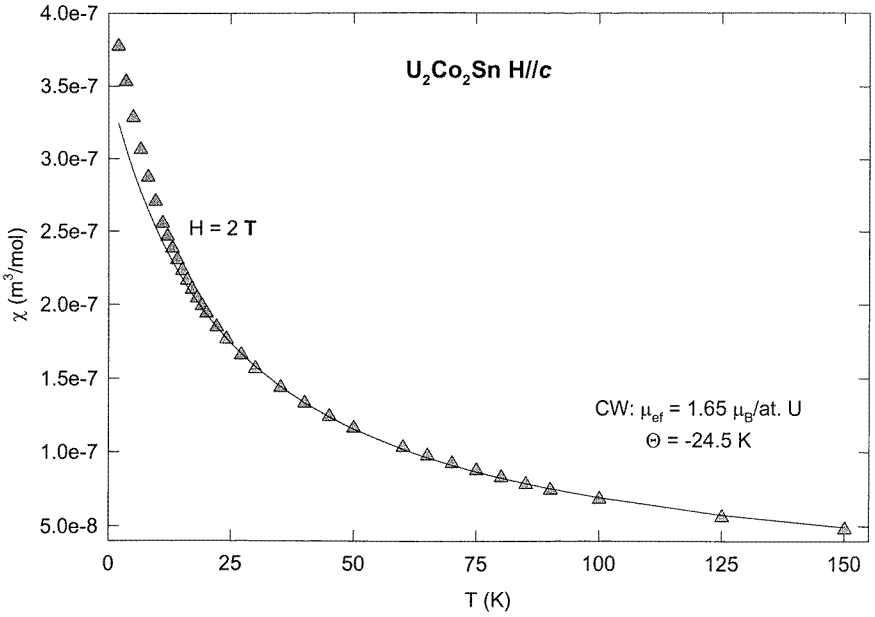

Figure 2. The temperature dependence of the susceptibility measured with a field of 2 T applied along the *c*-axis. The solid curve shows the fit of the Curie–Weiss law at high temperature.

for the *c*-direction. This difference indicates the presence of spin fluctuations, in agreement with results obtained with polycrystalline samples (Havela *et al* 1995).

3. Neutron scattering

The neutron scattering experiments were performed at the Centre d'Études Nucleaires de Grenoble, France (unpolarized neutrons) and at the Laboratoire Léon-Brillouin (LLB) in Saclay (polarized neutrons). The two experiments were performed on the same single crystal which has approximate dimensions $5 \times 3 \times 1$ mm^3.

3.1. Unpolarized neutrons

A set of 1826 integrated reflections were measured at room temperature on the four-circle neutron diffractometer DN4 of the Siloë reactor at the CEN, Grenoble. A Cu(220) monochromator was used to select a wavelength of $\lambda = 1.1798$ Å from the thermal beam. The $\lambda/2$ contamination of the monochromated beam was estimated to be of the order of 5×10^{-3}. The orientation matrix was refined from the angular settings of 20 strong and well centred reflections in the angular range $20.8^\circ \leqslant 2\theta \leqslant 86.6^\circ$. The cell parameters ($a = b = 7.298(5)$ Å, $c = 3.512(2)$ Å) are in good agreement with the values reported from single-crystal x-ray data (Péron *et al* 1993). The measured data-set extended out to $\sin(\theta)/\lambda = 0.625$ Å^{-1}. For each reflection a minimum of four equivalent reflections were measured, in order to improve the counting statistics and to check for anisotropic extinction effects. The intensity of the (220) reflection was measured every 3 h to monitor the stability of the experimental conditions. No significant decay of the intensity was noticed during the data collection. The reflection profiles were measured in ω–2θ scans. The integrated

intensities were derived from the profiles according to the Lehmann and Larson procedure (Lehmann and Larson 1974). The quality of the data collection is demonstrated by the internal agreement factors of the repeated measurements and symmetry-equivalent reflections, 1.07% and 1.22%, respectively. The excellent agreement between equivalent reflections rules out the possibility of the existence of significant anisotropic extinction. No absorption correction was performed ($\mu = 0.0963$ mm^{-1}). A unique data-set of 114 intensities was obtained after averaging symmetry-equivalent reflections. These were used in the least-squares refinement of the crystallographic structure.

3.2. Polarized neutrons

The polarized-beam experiment was performed on the 5C1 polarized-neutron diffractometer at the LLB, using the same crystal as had been used for the crystallographic study. The crystal was mounted with the c-axis vertical, parallel to the ω-axis of the instrument and to the applied magnetic field which was supplied by an asymmetric split-coil superconducting magnet. The 5C1 diffractometer works in normal-beam geometry, so reflections with scattering vectors out of the equatorial plane can be measured by tilting the detector. The beam coming from the hot-neutron source is monochromatized ($\lambda = 0.843$ Å) and simultaneously polarized by Bragg reflection from a (111) face of a Heusler single crystal. The polarization of the incoming beam was extracted before starting the experiment from the measured flipping ratio of the (200) reflection from a small FeCo crystal and found to be $p = 0.942(5)$. An Er filter was inserted in the incoming beam path to reduce the $\lambda/2$ contamination to less than 4×10^{-3}. Inversion of the neutron polarization was achieved by means of a Meissner–Majorana cryoflipper with an efficiency close to 100%. All data were taken at a stabilized temperature of 2 K and in an applied magnetic field of 5.5 T. During the experiment the flipping ratios of 373 Bragg reflections were measured, out to $\sin(\theta)/\lambda = 0.6$ Å^{-1}. For each reflection, at least four symmetry equivalents were measured and in some cases the measurements were repeated two or three times in order to improve the counting statistics. The magnetic structure factors were derived from the values of the measured flipping ratios using the standard Cambridge procedure. For data reduction, we have used the set of CCSL programs ARRNGE and SORGAM (Brown and Matthewman 1987). The usual corrections, including those for incomplete beam polarization and extinction, were applied to the data when extracting the magnetic structure factors from the flipping ratios. After averaging symmetry-equivalent reflections, a set of 39 unique magnetic structure factors were obtained; of these, 33 had $F_{mag} > \sigma$ and were used in the magnetization density study.

Table 1. Atomic positions and anisotropic displacement parameters (in units of 10^{-4} Å^2). The cell parameters at room temperature are $a = 7.298(5)$ Å, $c = 3.512(2)$ Å.

	x	y	z	U_{11}	U_{22}	U_{33}	U_{12}	Site
U (4h)	0.1713(1)	$x + 1/2$	1/2	80(6)	80(6)	60(7)	4(3)	1.00
Co (4g)	0.3703(4)	$x + 1/2$	0	75(2)	75(2)	13(2)	0(1)	0.94(2)
Sn (2a)	0	0	0	77(9)	77(9)	87(12)	0	1.00(2)

4. Structure refinement

The crystallographic structure of U_2Co_2Sn was refined using the room temperature data-set of integrated intensities. The least-squares program used in the calculations was a locally modified version of SFLSQ (Brown and Matthewman 1987). The quantity minimized by least-squares

fitting was $\sum w(|F_o|-|F_c|)^2$ where F_o and F_c are the observed and calculated nuclear structure factors, and w is the weight assigned to each reflection. We have used $w = 1/\sigma^2$, with σ derived from counting statistics following the McClandish procedure: $\sigma_I^2 = \sigma_s^2 + (pF_o^2)^2$. The parameter $p = 0.015$ is used to downweight the strongest reflections, by taking it into account that a small percentage of the variance should be added to the statistical error to take into account instrumental stabilities (McClandish *et al* 1975). The neutron scattering lengths used in the calculations are those compiled by Koester *et al* (1991): $b_{\mathrm{U}} = 8.417$ fm, $b_{\mathrm{Co}} = 2.49$ fm, $b_{\mathrm{Sn}} = 6.225$ fm. An extinction correction based on the formalism of Becker and Coppens (1974) was included in the model, although extinction is very small in our crystal, as shown below. The refined parameters include the U and Co atomic positions (x_{U}, x_{Co}), the anisotropic thermal displacement parameters of the three atoms, one scale factor, one extinction parameter (η) and the site occupancies of the Co and Sn atoms (14 variables). After a few least-squares cycles the refinement converged to the values given in table 1. The agreement between the calculated and measured scattering amplitudes is very good; the residual factors are $R(F) = 2.67\%$, $R_w(F) = 2.86\%$. The only remarkable features of the structural refinement are the anisotropic thermal motion of the Co atoms which vibrate more strongly on the *a–b* plane and a probable small deviation from the ideal stoichiometry for Co at the 4g site with an occupation of 0.94(2).

The average loss of intensity due to extinction effects is small, only 2%, the most strongly affected reflection having a reduction of 13% of intensity at $\lambda = 1.178$ Å. This is in agreement with the relatively large value of $\eta = 0.15'$ obtained for the half-width of the mosaicity distribution given by the least-squares refinement.

5. Magnetization density

An analysis of the magnetization density distribution was performed by least-squares fitting the measured magnetic structure factors derived from the polarized-neutron data to a simple model assuming spherical magnetization densities located at the sites occupied by the actinide and transition metal atoms.

The magnetic structure factors, $F_M(hkl)$, are the Fourier components of the magnetization density distribution in the crystal, and can be calculated in this model as

$$F_M(hkl) = \sum_{j=1}^{n} \mu_j s_j f_j(Q) \mathrm{e}^{2\pi \mathrm{i}(hx_j+ky_j+lz_j)} \mathrm{e}^{-W_j}.$$

In this expression the sum extends over the n magnetic sites, μ_j is the moment of the atoms

Table 2. Atomic moments on U_2Co_2Sn derived from the analysis of the polarized-neutron diffraction data. The results for two models (I and II) are shown. Model I has two parameters (μ(U), μ_L(U)) and the Co atoms have no moment, whereas model II includes as an additional parameter: the moment of the Co atoms. See also table 3.

Site	I	II
U (4h), μ	0.106(4)	0.118(3)
U (4h), μ_L	0.218(12)	0.200(8)
Co (4g)	—	0.013(2)
C_2	2.05(13)	1.69(8)
$-\mu_L/\mu_S$	1.9(2)	2.4(3)
χ^2	4.70	1.91

Table 3. Polarized-neutron data. F_o and F_c are the observed and calculated magnetic structure factors, respectively. The calculated data correspond to model II with the best-fit parameters given in table 2.

h	k	l	$\sin(\theta)/\lambda$	F_o	F_c	$\sigma(F_o)$
2	0	0	0.137	−0.230	−0.232	0.005
4	0	0	0.274	−0.151	−0.142	0.007
6	0	0	0.411	0.133	0.163	0.008
2	1	0	0.153	0.270	0.269	0.003
3	1	0	0.217	0.187	0.183	0.005
4	1	0	0.283	−0.221	−0.227	0.009
6	1	0	0.417	−0.014	0.034	0.06
8	1	0	0.553	0.065	0.048	0.016
2	2	0	0.194	0.097	0.112	0.006
3	2	0	0.247	0.055	0.042	0.011
4	2	0	0.307	0.069	0.057	0.006
5	2	0	0.369	0.136	0.118	0.013
7	2	0	0.499	−0.096	−0.086	0.011
8	2	0	0.565	0.026	0.027	0.016
3	3	0	0.291	−0.286	−0.288	0.009
5	3	0	0.400	0.103	0.100	0.012
7	3	0	0.522	0.033	0.033	0.014
4	4	0	0.388	0.048	0.044	0.013
5	4	0	0.439	−0.116	−0.101	0.013
7	4	0	0.553	0.078	0.067	0.021
6	5	0	0.535	−0.091	−0.016	0.067
6	6	0	0.582	0.059	0.062	0.018
2	0	1	0.198	0.187	0.201	0.012
4	0	1	0.309	0.106	0.080	0.011
6	0	1	0.435	−0.133	−0.141	0.03
2	1	1	0.209	−0.293	−0.288	0.012
4	1	1	0.316	0.200	0.204	0.012
5	1	1	0.377	0.021	0.063	0.015
5	2	1	0.396	−0.134	−0.128	0.012
6	2	1	0.456	0.079	0.071	0.013
7	2	1	0.519	0.100	0.070	0.03
3	3	1	0.324	0.236	0.230	0.011
5	4	1	0.461	0.112	0.092	0.013

at the j-site, s_j is the site occupation and W_j is the Debye–Waller factor. The function $f(Q)$ is the magnetic form factor, which is the Fourier transform of the magnetization density associated with a single atom. The uranium magnetic form factor was calculated in the dipole approximation (Marshall and Lovesey 1971):

$$\mu f(Q) = \mu(\langle j_0\rangle + C_2\langle j_2\rangle) \qquad C_2 = \frac{\mu_L}{\mu}$$

where the C_2-coefficient is the ratio between the orbital (μ_L) and total (μ) moments of the actinide atom. The $\langle j_0\rangle$ and $\langle j_2\rangle$ functions were derived from the radial wave-functions calculated by Desclaux and Freeman (1978) for a U^{3+} ion using a fully relativistic code. For the transition metal atom, a spin-only form factor was used which was calculated from the atomic wave-functions of Clementi and Roetti (1974).

Two refinements of the model were performed. In refinement I the Co atoms were assumed to have no magnetic moment and only two parameters were refined, the total uranium moment and the C_2-coefficient. In refinement II, the Co atoms were allowed to polarize, and the model

includes as an additional parameter the value of the magnetic moment carried by the Co atom. The results of the two refinements are shown in table 2. Both models give a satisfactory agreement with the measured data, but the fit is better when a small moment at the Co site is included. The decrease in χ^2 from 4.70 to 1.91 is statistically significant even if model II includes an additional parameter compared to model I. As will be shown below, a maximum-entropy reconstruction of the magnetization density in the unit cell also supports the existence of a small magnetic moment at the transition metal atom.

The measured value of the C_2-coefficient in refinement II is 1.69(8) which is close to the standard value (1.64) of a U^{3+} ion calculated for an intermediate-coupling configuration. From the C_2-coefficient the ratio between the orbital and spin moments of the actinide atom can be calculated as

$$-\mu_L/\mu_S = \frac{C_2}{C_2 - 1}$$

which is a parameter that previous studies have shown to be systematically smaller than the free-ion value in strongly hybridized 5f actinide intermetallics (Lebech *et al* 1991). We have obtained a value $-\mu_L/\mu_S = 2.4(3)$ which is not far from the free-ion value for U^{3+} (2.56). The accuracy of this parameter is affected by the fact that the least-squares correlation matrix shows a relatively large (70%) correlation between the parameters describing the uranium moment value and its orbital component. The value of the cobalt moment, on the other hand, does not correlate significantly with the other parameters of the model.

A more direct insight into the magnetization density distribution in the unit cell can be obtained by Fourier transforming the magnetic structure factor amplitudes. However, the series termination effect is a serious drawback of this method, particularly when small details of the magnetization density are to be analysed. This problem can be avoided by calculating a difference Fourier series convoluted with a suitable apodizing function, at the cost of a loss of spatial resolution. Another possibility, that does not suffer from this drawback, is to use the maximum-entropy method to reconstruct the magnetization density (Papoular and Gillon 1990). This method provides a less noisy magnetization density map compatible with the measured data within the error bars. We have used the maximum-entropy code of Kumazawa, Kubota and Sakata (Sakata and Sato 1990, Sakata *et al* 1990, 1993) in a version adapted for the LINUX operating system by Burger and Prandl (1997). The calculation was performed on a grid of $48 \times 48 \times 32$ pixels and the prior density was chosen to be a flat distribution with a value equal to the average magnetization density in the cell as given by the SQUID measurements.

As the polarized-neutron data were collected in normal-beam geometry with the magnetic field parallel to the c-axis, only a limited set of (hkl) reflections with $l \neq 0$ could be measured. This means that the resolution of the reconstructed magnetization density along the c-axis is poor. The best resolution is achieved in a projection on the (001) plane of the magnetization density, where both the uranium and cobalt atoms are well resolved. The maximum-entropy map of this projection is shown in figure 3. In addition to the large peaks at the actinide positions, small peaks are also observed at the positions occupied by the Co atoms, confirming that both U and Co atoms polarize under the applied field, although the moment on the Co atoms is much smaller, in agreement with the results of table 1.

6. Discussion

The purpose of this work was to address the interplay between hybridization and magnetism in the U_2T_2X system, after having chosen a compound, U_2Co_2Sn, for which hybridization between the d and f states is strong enough to suppress magnetic ordering. We have used the

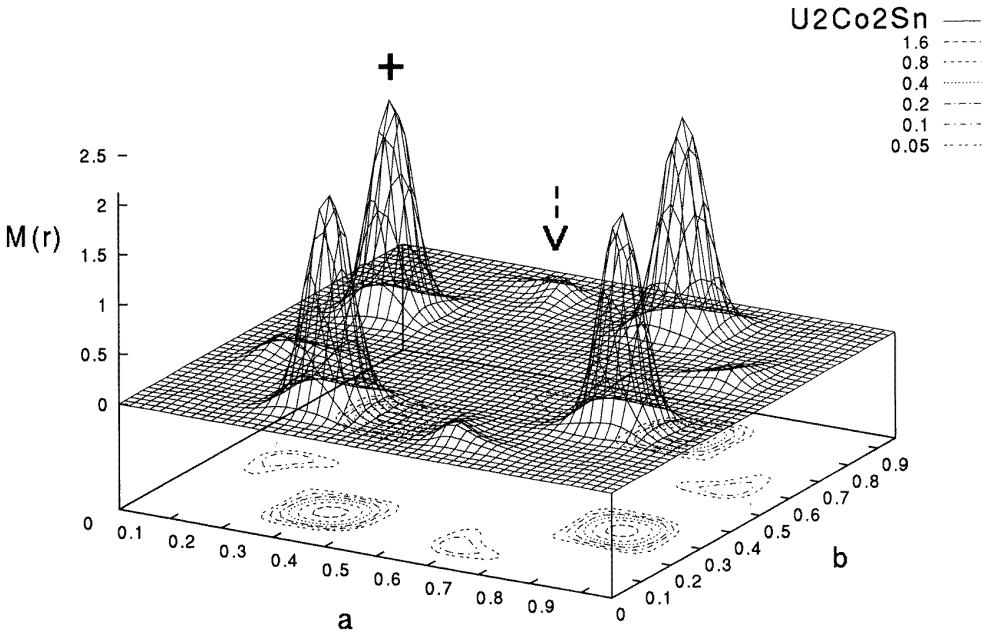

Figure 3. A magnetization density map of U_2Co_2Sn showing the projection of the magnetization density distribution on the *a–b* plane reconstructed by the maximum-entropy method from the polarized-neutron scattering data. The position of one uranium atom and one cobalt atom are indicated by a cross and an arrow, respectively. The other peaks correspond to symmetry-equivalent positions.

high sensitivity of polarized-neutron scattering to study the small magnetization induced by a strong magnetic field applied along the easy axis. This technique probes the magnetization density distribution with atomic resolution providing the individual site susceptibilities which should be compared with theoretical calculations in an effort to develop systematics for this interesting family of compounds.

The single-crystal magnetization data reported here support the view of U_2Co_2Sn as a spin fluctuator that remains paramagnetic down to 2 K and which has a large uniaxial magnetic anisotropy. Pinto *et al* (1995) have reported resistivity and thermopower measurements on polycrystalline samples. They have found a maximum in $\mathrm{d}\rho/\mathrm{d}T$ at around 12.5 K and another anomaly in the resistivity at 100 K. The high-temperature anomaly was also observed by these authors on the basis of thermopower measurements. In our magnetization and susceptibility measurements these anomalies were not found.

At 2 K and 5.5 T the induced magnetization along the *c*-axis is 220 $\mathrm{m}\mu_\mathrm{B}$/f.u. to be compared with a value of 262(7) $\mathrm{m}\mu_\mathrm{B}$/f.u. determined by neutron scattering. The difference is likely to be attributable to a negative conduction electron polarization. The magnetic scattering due to the polarization of the highly delocalized conduction electrons will only be significant at small Q, and therefore cannot be measured directly in a conventional diffraction experiment. In light rare-earth and actinide systems the conduction electrons are polarized antiparallel to the local moment and this fact is well understood. In ferromagnetic materials such as US (Wedgwood 1972) or UFe_2 (Lebech *et al* 1989) the moment due to conduction electron polarization attains values of the order of 10% of the total moment. The value of $\sim$20% found for U_2Co_2Sn is a bit larger, but not far outside the range of expected values. One cannot exclude

the possibility that a small misorientation of the easy axis with respect to the field during the SQUID measurements could explain part of the difference between the magnetization and neutron scattering values, but we estimate that this error should not exceed 5%.

For most uranium intermetallic compounds, it has been found that the U moments are aligned perpendicular to the direction of nearest-neighbour U–U bonds. The commonly accepted physical explanation for this is that uranium 5f electrons hybridize strongly in these directions and the associated orbital moment is then oriented perpendicular to these bonds. However, if the dominant hybridization is that between the f electrons and d-electron states of the ligands, a similar reasoning would imply that the relevant distances are the shortest U–T bonds. In U_2Co_2Sn the shortest U–U distances join two atoms along the c-axis (3.512 Å); the second neighbours are in the plane at a slightly larger distance (3.536 Å). One would therefore expect a weak, basal-plane anisotropy if direct 5f–5f hybridization were the determining factor.

The polarized-neutron data show that a small part of the induced magnetization is due to the Co atoms, with a local susceptibility that is about 10% of that of the uranium atom. Cobalt is itself a magnetic element, but band-structure calculations reported by Diviš *et al* (1995) for U_2Co_2Sn show that the covalency gap exceeds the energy of exchange splitting of Co atoms and no spontaneous magnetic polarization of T d electrons is expected. Thus, the observation of an induced magnetic moment at the Co sites shows that some degree of hybridization must exist between the f and d electrons, with a small magnetic moment transferred to the transition metal atoms.

A crystal-field analysis of the band-structure calculations suggests that the transition metal orbitals mixing with the U(f) states at E_F are predominantly of the form $3xy^2-y^3$ and x^3-3xy^2. The experimental magnetization density map shows a small magnetic moment located at the Co sites, but details of the magnetization density, e.g., asphericities in the magnetization distribution, could not be resolved in our experiment.

Matar (1995) has also reported a detailed band-structure LDA calculation of U_2T_2Sn (T = Fe, Co, Ni) using the augmented-spherical-wave method in both unpolarized and spin-polarized configurations. A charge transfer from the transition metal to the actinide atoms was found in both U_2Fe_2Sn and U_2Co_2Sn, with a magnitude that is almost twice as large for the former, while the departure of Sn from neutrality is negligible. This was considered as indicative of a strong covalent interaction between Fe and U and, to a lesser extent, between Co and U. The charge transfer for U_2Ni_2Sn is very small. According to Matar (1995), these charge transfers cannot be explained by a different overlap between the atomic spheres due to a change in lattice parameters and should be ascribed to hybridization between the transition metal and U states. The calculated densities of states show that the predominant orbitals at E_F have 5f character. The bonding and antibonding bands consist mainly of T d and U 5f states, respectively. There is, however, an appreciable amount of covalency, with U 5f contributing to the bonding states and T d to the antibonding states. Such a hybridization would result in a small polarization of the transition metal atoms, as reported in this study for U_2Co_2Sn. A similar situation occurs for UCoAl, where small moments on the cobalt sites were also found by polarized-neutron scattering (Papoular and Delapalme 1994). The hybridization is also strong enough to suppress magnetic ordering in this compound, which behaves as a paramagnet at low temperatures and small fields but has a metamagnetic transition to an ordered state.

Although band-structure calculations correctly predict the magnetic ground state of both U_2Fe_2Sn and U_2Ni_2Sn, as paramagnetic and magnetically ordered, respectively, for U_2Co_2Sn there is only a small energy difference between the spin-polarized and non-spin-polarized configurations. A local minimum corresponding to small, albeit finite, magnetic moments was found, only slightly displaced form the true zero-moment minimum. Low-energy excitations may therefore play an important role in the magnetic ground state of U_2Co_2Sn, and indeed

the calculations support the picture of U_2Co_2Sn as a spin fluctuator. It would certainly be interesting to extend these types of study using polarized neutrons to U_2Fe_2Sn which is a more strongly hybridized system, to determine the relative magnetic susceptibilities of the actinide and transition metal atoms and the nature of the hybridized wave-functions.

Acknowledgments

This work is part of a project financed by JNICT under contract PBIC/FIS/2213/95. J A Paixão and L C J Pereira acknowledge the European Union (EU) for support given within the framework of the 'Human Capital and Mobility Programme' allowing them to perform the neutron scattering experiments at Silöe and Saclay.

References

Becker P J and Coppens P 1974 *Acta Crystallogr.* A **30** 129
Brown P J and Matthewman J C 1987 The Cambridge Crystallographic Subroutine Library—Mark 3 users's manual *Rutherford Appleton Laboratory Internal Report* RAL-87-010
Burger K and Prandl W 1997 *Z. Kristallogr.* **212** 493
Clementi E and Roetti C 1974 *At. Data Nucl. Data Tables* **14** 178
Desclaux J P and Freeman A J 1978 *J. Magn. Magn. Mater.* **8** 119
Diviš M, Olšovec M, Richter M and Eschrig H 1995 *J. Magn. Magn. Mater.* **140–144** 1365
Diviš M, Richter M and Eschrig H 1994 *Solid State Commun.* **90** 99
Diviš M, Richter M and Eschrig H 1997 *J. Alloys Compounds* **255** 11
Fukushima T, Kumada T, Matsuyama S, Kindo K, Prokeš K, Nakotte H, de Boer F R, Havela L, Sechovský V, Winand J M, Rebizant J and Spirlet J C 1995 *Physica* B **211** 142
Havela L, Sechovský V, Svoboda P, Diviš M, Nakotte H, Prokeš K, de Boer F R, Purwanto A, Robinson R A, Seret A, Winand J M, Rebizant J, Spirlet J C, Richter M and Eschrig H 1994 *J. Appl. Phys.* **76** 6214
Havela L, Sechovský V, Svoboda P, Nakotte H, Prokeš K, de Boer F R. Seret A, Winand J M, Rebizant J, Spirlet J C, Purwanto J C and Robinson R A 1995 *J. Magn. Magn. Mater.* **140–144** 1367
Koester L, Rauch H and Seymann E 1991 *At. Data Nucl. Data Tables* **49** 65
Lebech B, Wulff M and Lander G H 1991 *J. Appl. Phys.* **69** 5891
Lebech B, Wulff M, Lander G H, Rebizant J, Spirlet J C and Delapalme A 1989 *J. Phys.: Condens. Matter* **1** 10 229
Lehmann M S and Larson F K 1974 *Acta Crystallogr.* A **30** 580
Marshall W and Lovesey S W 1971 *Theory of Neutron Scattering from Condensed Matter* (London: Oxford University Press)
Matar S F 1995 *J. Magn. Magn. Mater.* **151** 263
McClandish L E, Stout G H and Andrews L C 1975 *Acta Crystallogr.* A **31** 245
Mirambet F, Gravereau P, Chevalier B, Trut L and Etourneau J 1993 *J. Alloys Compounds* **191** L1
Nakotte H, Prokěs K, Brück E, Tang N, de Boer F R, Svoboda P, Sechovský V, Havela L, Winand J M, Seret A, Rebizant J and Spirlet J C 1994 *Physica* B **201** 247
Paixão J A, Lander G H, Brown P J, Nakotte H, de Boer F R and Brück E 1992 *J. Phys.: Condens. Matter* **4** 829
Paixão J A, Lander G H, Delapalme A, Nakotte H, de Boer F R and Brück E 1993 *Europhys. Lett.* **24** 607
Papoular R J and Delapalme 1994 *Phys. Rev. Lett.* **72** 1486
Papoular R J and Gillon B 1990 *Europhys. Lett.* **13** 439
Pereira L C J, Paixão J A, Estrela P, Godinho M, Boudarot F, Bonnet M, Rebizant J, Spirlet J C and Almeida M 1996 *J. Phys.: Condens. Matter* **8** 11 167
Péron M N, Kergadallam Y, Rebizant J, Meyer D, Winand J M, Zwirner S, Havela L, Nakotte H, Spirlet J C, Kalvius G M, Colineau E, Oddou J L, Jeandey C and Sanchez J P 1993 *J. Alloys Compounds* **201** 203
Pinto R P, Amado M M, Salgueiro M A, Braga M E, Sousa J B, Chevalier B, Mirambet F and Étourneau J 1995 *J. Magn. Magn. Matter.* **140–144** 1371
Sakata M, Mori R, Kumazawa S, Takata M and Toraya H 1990 *J. Appl. Crystallogr.* **23** 526
Sakata M and Sato M 1990 *Acta Crystallogr.* A **46** 263
Sakata M, Uno M and Takata M 1993 *J. Appl. Crystallogr.* **26** 159
Wedgwood F A 1972 *J. Phys. C: Solid State Phys.* **5** 2427